

Samir Softic,^{1,2} Jeremie Boucher,¹ Marie H. Solheim,^{1,3} Shiho Fujisaka,¹
Max-Felix Haering,¹ Erica P. Homan,¹ Jonathon Winnay,¹ Antonio R. Perez-Atayde,⁴
and C. Ronald Kahn¹



Lipodystrophy Due to Adipose Tissue-Specific Insulin Receptor Knockout Results in Progressive NAFLD



Diabetes 2016;65:2187–2200 | DOI: 10.2337/db16-0213

Ectopic lipid accumulation in the liver is an almost universal feature of human and rodent models of generalized lipodystrophy and is also a common feature of type 2 diabetes, obesity, and metabolic syndrome. Here we explore the progression of fatty liver disease using a mouse model of lipodystrophy created by a fat-specific knockout of the insulin receptor (F-IRKO) or both IR and insulin-like growth factor 1 receptor (F-IR/IGFRKO). These mice develop severe lipodystrophy, diabetes, hyperlipidemia, and fatty liver disease within the first weeks of life. By 12 weeks of age, liver demonstrated increased reactive oxygen species, lipid peroxidation, histological evidence of balloon degeneration, and elevated serum alanine aminotransferase and aspartate aminotransferase levels. In these lipodystrophic mice, stored liver lipids can be used for energy production, as indicated by a marked decrease in liver weight with fasting and increased liver fibroblast growth factor 21 expression and intact ketogenesis. By 52 weeks of age, liver accounted for 25% of body weight and showed continued balloon degeneration in addition to inflammation, fibrosis, and highly dysplastic liver nodules. Progression of liver disease was associated with improvement in blood glucose levels, with evidence of altered expression of gluconeogenic and glycolytic enzymes. However, these mice were able to mobilize stored glycogen in response to glucagon. Feeding F-IRKO and F-IR/IGFRKO mice a high-fat diet for 12 weeks accelerated the liver injury and normalization of blood glucose levels. Thus, severe fatty liver disease

develops early in lipodystrophic mice and progresses to advanced nonalcoholic steatohepatitis with highly dysplastic liver nodules. The liver injury is propagated by lipotoxicity and is associated with improved blood glucose levels.

Nonalcoholic fatty liver disease (NAFLD) is a common manifestation of diabetes, obesity, and metabolic syndrome. NAFLD also occurs in human and rodent models of lipodystrophy (1–4). In the context of obesity and metabolic syndrome, NAFLD may progress to include liver inflammation or nonalcoholic steatohepatitis (NASH), fibrosis, and occasionally, hepatocellular carcinoma (5), whereas not much is known about the natural history of liver disease in the context of lipodystrophy.

Metabolic syndrome is present in 80% of patients with lipodystrophy, almost universally manifesting as severe insulin resistance, profound hypertriglyceridemia, and ectopic lipid accumulation (6). One major difference between this form of metabolic syndrome and that associated with obesity is in the amount of adipose tissue, which is reduced in lipodystrophy, resulting in low levels of leptin (7), whereas obesity is associated with increased adiposity and high leptin levels. In regards to other metabolic outcomes, including ectopic fat accumulation in the liver, lipodystrophy resembles an extreme version of the obesity-associated metabolic syndrome (8).

¹Section on Integrative Physiology and Metabolism, Joslin Diabetes Center and Department of Medicine, Harvard Medical School, Boston, MA

²Division of Gastroenterology, Hepatology and Nutrition, Boston Children's Hospital, Boston, MA

³Department of Clinical Science, KG Jebsen Center for Diabetes Research, University of Bergen, Bergen, Norway

⁴Department of Pathology, Boston Children's Hospital, and Harvard Medical School, Boston, MA

Corresponding author: C. Ronald Kahn, c.ronald.kahn@joslin.harvard.edu.

Received 11 February 2016 and accepted 29 April 2016.

This article contains Supplementary Data online at <http://diabetes.diabetesjournals.org/lookup/suppl/doi:10.2337/db16-0213/-/DC1>.

S.S. and J.B. contributed equally to this work.

J.B. is currently affiliated with Cardiovascular and Metabolic Diseases iMed, AstraZeneca R&D, Mölndal, Sweden.

© 2016 by the American Diabetes Association. Readers may use this article as long as the work is properly cited, the use is educational and not for profit, and the work is not altered.

See accompanying article, p. 2201.

Whether lipid accumulation in the liver is a sign of a disease or a physiologic response in patients who have minimal capacity to store lipids in the adipose tissue is unknown. In lipodystrophic patients, the liver fat decreases with leptin treatment (9,10), suggesting that at least a portion of stored liver fat may be used for ketogenesis (11). What processes mediate ketogenesis in the setting of minimal adipose tissue lipid stores are unknown, but it is interesting to note that serum levels of the ketogenic hormone, fibroblast growth factor 21 (FGF21), are elevated with lipodystrophy in patients infected with HIV-1 (12) and that the liver is the main source of elevated serum FGF21 levels in mice with lipodystrophy (13).

The liver disease in some patients with generalized lipodystrophy can progress to liver cirrhosis requiring liver transplantation (14). The most characteristic feature of fatty liver disease associated with lipodystrophy is prominent steatosis with hepatocyte balloon degeneration (8,15), pointing to lipotoxicity as an important pathway of liver injury. Chronic liver injury resulting in cirrhosis and liver failure can be associated with reduced hepatic glucose production leading to hypoglycemia (16). What effects liver lipotoxicity may have on hepatic glucose homeostasis in the setting of lipodystrophy is unknown.

Here, we show that mice lacking insulin receptor (IR) or both IR and insulin-like growth factor 1 receptor (IGF1R) in adipose tissue display a lipodystrophic phenotype associated with severe diabetes and NAFLD. The liver disease in these mice progresses to NASH, fibrosis, and highly dysplastic liver nodules. Interestingly, this progressive liver disease is associated with improvement of hyperglycemia in these mice with age, despite the persistent insulin resistance and a normal ability to mobilize stored glycogen in response to glucagon. The liver injury in these lipodystrophic mice is propagated by lipotoxicity, and high-fat diet (HFD) feeding accelerates the progression of liver disease, leading to normalization of blood glucose levels.

RESEARCH DESIGN AND METHODS

All protocols were approved by the Joslin Diabetes Center Institutional Animal Care and Use Committee and were in accordance with National Institutes of Health guidelines.

Animals and Diets

Fat-specific IR, IGF1R, and IR/IGF1R knockout (KO) mice (F-IRKO, F-IGFRKO, and F-IR/IGFRKO mice, respectively) were generated as described (17). Mice were housed at 20–22°C on a 12-h light/dark cycle with ad libitum access to water and food. For the HFD experiments, the mice were fed a chow diet (Mouse Diet 9F, PharmaServ) until 8 weeks of age and then were continued on chow or switched to a 60% HFD (D12492, Research Diets) for an additional 12 weeks.

Glucose Tolerance Tests and Glucagon Response

Glucose tolerance tests were performed on overnight fasted mice injected with dextrose (2 mg/g i.p.). Glucagon response was assessed in mice fasted overnight injected

with glucagon (1 unit/kg; G2044, Sigma-Aldrich) with blood glucose measured at 0, 15, 30, 60, and 120 min. Glucose levels were measured using an Infinity glucose meter (US Diagnostics).

Tissue and Serum Analyses

Tissues were stored frozen or fixed in formalin, and sections were stained with hematoxylin and eosin (H&E) or periodic acid Schiff (PAS). mRNA extraction and quantification was performed as previously described (18). Serum parameters were determined by the Joslin Diabetes Research Center assay core using commercial kits. Hormones were assessed by ELISA, adipokines were measured by a multiplex assay, and alanine aminotransferase (ALT) and aspartate aminotransferase (AST) were assessed by colorimetric assays. Triglycerides from liver samples were measured with a triglyceride quantification kit (Abnova), as previously described by Debosch et al. (19).

Protein Extraction and Immunoblot Analysis

Tissues were homogenized in radioimmunoprecipitation assay buffer (EMD Millipore) with protease and phosphatase inhibitor cocktail (BioTools). Proteins were separated using SDS-PAGE and transferred to polyvinylidene difluoride membrane (Millipore). Immunoblotting was performed using the indicated antibodies: phosphorylated (p)-IR/IGFR (#3024) and p-phosphatase and tensin homolog (PTEN) (#9552) from Cell Signaling Technologies and IR (#SC-711), PTEN (#SC-9145) and actin (SC-1616) from Santa Cruz Biotechnology. Quantification of immunoblots was performed using ImageJ software (National Institutes of Health).

Immunohistochemistry and Immunofluorescence

Immunohistochemistry (IHC) was performed on formalin-fixed sections and immunofluorescence (IF) on frozen sections. In brief, paraffin-embedded, formalin-fixed sections were deparaffinized and rehydrated. Antigen was recovered by boiling in citrate buffer (H-3300, Vector Laboratories) and incubation in Triton-X, and were digested with proteinase K. Sections were blocked in goat serum and incubated overnight at 4°C for IHC with primary antibodies against β catenin (D13A1, Cell Signaling), F4/80 (ab6640, Abcam), or 4-hydroxynonenal (4-HNE) (ab46545, Abcam). Subsequently, slides were incubated with biotinylated secondary antibody, and the reaction was developed using avidin/streptavidin horseradish peroxidase (PK-4001, Vector Laboratories). For IF, slides were incubated overnight with primary antibody against Ki67 (556003, Becton-Dickinson,) and phosphatidylinositol 3,4,5-trisphosphate (PIP₃) (P-0008, Echelon), followed by a secondary antibody labeled with Texas Red (Vector Laboratories) or Alexa Fluor (Invitrogen) and counterstained with DAPI mounting media (H-1500, Vector Laboratories). Dihydroethidium (DHE) stain was performed on frozen liver sections fixed with 4% paraformaldehyde and stained with a 1:1,500 dilution of DHE (10 μ g/mL) stain for 10 min at 37°C. Slides were washed twice in PBS and coverslipped. Images were captured using an Olympus BX60 fluorescence microscope.

In Vivo Glucose Uptake

After 12 weeks of the HFD, control, F-IRKO, and F-IR/IGFRKO mice were injected with glucose (2 mg/g i.p.) (D20) combined with 0.33 mCi [^{14}C]2-deoxyglucose per gram of body weight. After 15 min, [^{14}C] levels in the liver and quadriceps muscle were determined, as previously published (20).

Statistical Analyses

Data are presented as mean \pm SEM and were analyzed by unpaired two-tailed Student *t* test or ANOVA, as appropriate.

RESULTS

Lipodystrophic Mice Develop Fatty Liver Disease and Lipotoxicity

Mice with fat-specific KO of the IR, IGF1R, or both, were generated by breeding mice with IR and IGF1R floxed alleles (18) and mice carrying a Cre-recombinase transgene driven by the adiponectin promoter (21). Whereas KO of the IGF1R had minimal effect on white and brown fat development, F-IRKO and F-IR/IGFRKO mice displayed virtually from birth a profound reduction in weights of subcutaneous and visceral white adipose tissue depots (17). Lipodystrophy was associated with hyperglycemia (Fig. 1A) and severe diabetes at 12 weeks of age. At this time, liver weights of both F-IRKO and F-IR/IGFRKO mice were increased four- to fivefold above the control, whereas the liver weight of F-IGFRKO mice remained normal (Fig. 1B). Hepatomegaly in F-IRKO and F-IR/IGFRKO mice was associated with a three- to fivefold increase in liver triglyceride accumulation (Fig. 1C and D). There were also two- to fivefold increases in the expression of genes, such as *Acc1*, *Fas*, and *Scd1*, involved in de novo lipogenesis (Fig. 1E). However, at this age, these mice did not display an increase in expression of *Tnf- α* , and *F4/80*, although there was some increase in the macrophage marker *CD11c* (Fig. 1F). F-IRKO and F-IR/IGFRKO mice also did not show significant fibrosis as assessed by trichrome, Sirius red, and reticulin stains (Supplementary Fig. 1), and mRNA levels of *Tgf- β* and *α Sma* were not elevated. *Col1a1* was increased in F-IR/IGFRKO mice; however, this may be a sign of stellate cell activation in the absence of other markers of fibrosis (22) (Fig. 1G). Histological assessment of liver at 12 weeks of age confirmed that lipodystrophic F-IRKO and F-IR/IGFRKO mice exhibited micro- and macrovesicular steatosis and the presence of balloon degeneration, with no significant inflammation or fibrosis (Table 1). Hepatocyte balloon degeneration is indicative of lipotoxicity and is associated with a progressive form of NAFLD (23,24). By 12 weeks of age, reactive oxygen species levels and lipid peroxidation, as assessed by DHE and 4-HNE stains, respectively, were also increased in the livers of F-IR/IGFRKO mice (Fig. 1H). F-IRKO and F-IR/IGFRKO mice exhibited decreased expression of one of the rate-limiting gluconeogenic enzymes *Pepck*, whereas the expression of *Fbp1* and *Pc* was actually increased compared with

the controls (Fig. 1I). Despite a decrease in *Pepck*, some gluconeogenic potential was likely preserved because these mice were hyperglycemic compared with the controls. Thus, lipodystrophic F-IRKO and F-IR/IGFRKO mice had profound hepatic steatosis and minimal signs of liver injury, which was primarily a result of lipotoxicity. F-IGFRKO mice, which did not develop lipodystrophy, did not exhibit any of these changes.

Lipodystrophic F-IRKO and F-IR/IGFRKO Mice Can Mobilize Stored Liver Fat

In addition to marked hepatosteatosis, lipodystrophic F-IRKO and F-IR/IGFRKO mice at 12 weeks of age exhibited serum dyslipidemia with elevated circulating triglyceride, cholesterol, and free fatty acid (FFA) levels (17). To determine to what extent these lipids could be mobilized, F-IRKO mice underwent a protocol of overnight fasting and an 8-h refeeding. Fasting resulted in a decrease in blood glucose levels in all mice, although the F-IRKO mice remained hyperglycemic compared with the controls (135 ± 13 vs. 87 ± 8 mg/dL), and refeeding resulted in a return to the marked hyperglycemic levels (Fig. 2A). Liver weight of F-IRKO mice also decreased by 38%, from 4.0 ± 0.4 to 2.5 ± 0.2 g, after fasting and returned to baseline (3.9 ± 0.2 g) after refeeding, demonstrating the ability of lipodystrophic mice to store and mobilize fat in the liver (Fig. 2B). Liver weight of control mice also decreased by fasting, from 1.1 ± 0.1 to 0.84 ± 0.02 g, and increased to 0.94 ± 0.07 g with refeeding. Serum triglyceride levels, which were elevated in randomly fed F-IRKO mice (230 ± 40 vs. 96 ± 10 mg/dL) decreased to levels even lower than control after an overnight fast (56 ± 7 vs. 108 ± 21 mg/dL), but then returned to baseline after refeeding (Fig. 2C). FFA levels increased with fasting in control mice from 0.7 ± 0.1 to 0.9 ± 0.0 mEq/L but, paradoxically, decreased in F-IRKO mice during fasting (1.2 ± 0.2 to 0.7 ± 0.1 mEq/L), probably reflecting the lack of adipose tissue lipolysis and increased FFA utilization in these mice (Fig. 2D). Insulin levels also decreased with fasting in control and F-IRKO mice, indicating normal pancreatic responses to nutrient intake and blood glucose levels (Fig. 2E). Likewise, β -hydroxybutyrate levels significantly increased with fasting in control and F-IRKO mice (Fig. 2F), suggestive of normal ketogenesis in lipodystrophic mice, despite the almost complete absence of white adipose tissue. Liver FGF21 mRNA was elevated in F-IRKO and F-IR/IGFRKO mice at every age tested (Fig. 2G).

F-IRKO and F-IR/IGFRKO Mice Develop Progressive NAFLD With Aging

The profound hepatomegaly present at 12 weeks of age was already evident by 2.5 weeks of age and continued to advance throughout the lifetime. By 52 weeks of age, livers in F-IRKO mice were 6.5 times heavier, and those in F-IR/IGFRKO mice were 9.2 times heavier than in the controls (Fig. 3A). Despite almost complete reduction of white adipose tissue in F-IRKO and F-IR/IGFRKO mice,

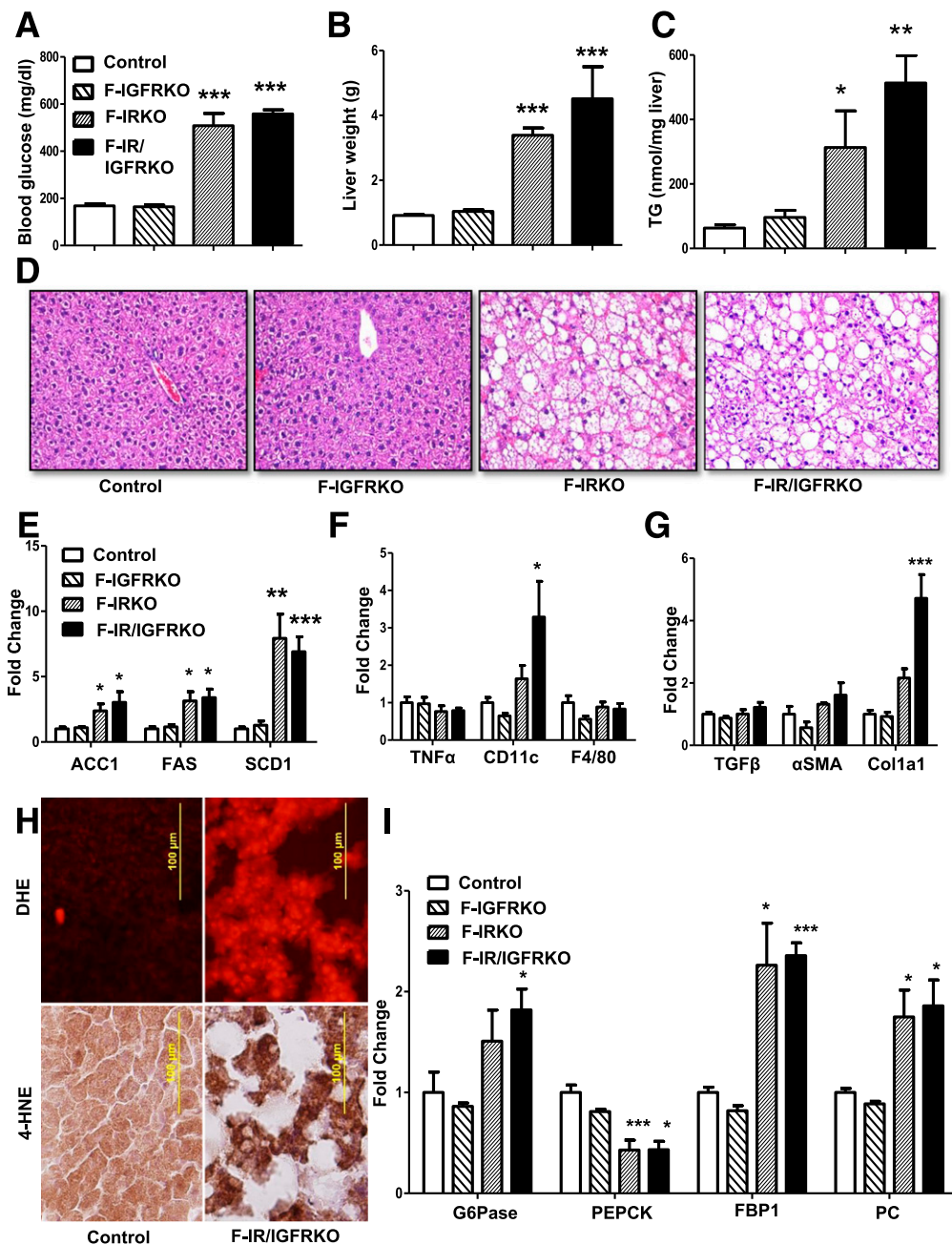


Figure 1—Fatty liver disease in 12-week-old lipodystrophic mice. Blood glucose (A), liver weight (B), and liver triglycerides (TG) (C) in 12-week-old, random-fed control, F-IGFRKO, F-IRKO, and F-IR/IGFRKO mice. Results are mean \pm SEM of 12 to 30 animals per group. D: Liver sections from the same mice stained with H&E. mRNA expression of genes involved in de novo lipogenesis (E), inflammation (F), and fibrosis (G) in the livers of 12-week-old control, F-IGFRKO, and F-IRKO mice. H: Liver sections from control and F-IR/IGFRKO mice stained with DHE and 4-HNE. I: Expression of gluconeogenic/glycolytic enzymes in the livers of chow-fed control, F-IGFRKO, F-IRKO, and F-IR/IGFRKO mice at 12 weeks of age. Results are mean \pm SEM of five to seven animals per group. * P < 0.05, ** P < 0.01, and *** P < 0.001 compared with controls.

and as a result of the massive hepatomegaly, body weight was not significantly different from the controls at up to 3 months of age and was actually 20% greater than the controls at 52 weeks of age (Fig. 3B). Hepatic triglycerides per milligram of tissue were also increased by three- to fivefold in F-IRKO and F-IR/IGFRKO mice as early as 2.5 weeks of age compared with controls and remained

elevated at 12 and 52 weeks of age (Fig. 3C). In parallel, steatosis was observed in F-IRKO and F-IR/IGFRKO mice at 2.5 weeks of age, which persisted at 12 and 52 weeks of age (Supplementary Fig. 2). This correlated with two- to threefold increases in the expression of enzymes involved in de novo lipogenesis (*Acc1*, *Fas*, and *Scd1*) in the lipodystrophic mice compared with controls at 2.5, 12, and

Table 1 — NAFLD activity scores

Genotype	Scale	Age							
		12 weeks			52 weeks				
		Wild-type	F-IGFRKO	F-IRKO	F-IR/IGFRKO	Wild-type	F-IGFRKO	F-IRKO	F-IR/IGFRKO
Macrovesicular steatosis	0-3	0	0	1.7 ± 0.4	2.6 ± 0.2	0.2 ± 0.2	0	2.8 ± 0.2	2.3 ± 0.2
Portal inflammation	0-3	0	0	0.4 ± 0.2	0	0	1.0 ± 0.0	0.6 ± 0.2	1.5 ± 0.2
Ballooning degeneration	0-2	0	0	1.9 ± 0.1	1.6 ± 0.2	0	0.2 ± 0.2	2.0 ± 0.0	1.3 ± 0.2
Interstitial fibrosis, stage	0-4	0	0	0.1 ± 0.1	0	0	0	0.8 ± 0.4	2.7 ± 0.2
Fibrosis present, % total		0	0	14	0	0	0	60	100

Results are mean ± SEM of 4 to 6 mice per group. NAFLD activity scores were assessed in H&E- and trichrome-stained liver sections of 12- and 52-week-old mice by a practicing clinical pathologist who adopted a modified version of a previously published method (40).

52 weeks of age. (Fig. 3D–F). Interestingly, the insulin-activated transcription factor *Srebp1c*, which regulates lipogenesis, was not elevated despite massive hyperinsulinemia (Supplementary Fig. 3).

Excessive lipid accumulation in the liver was associated with increased serum ALT in 5- and 12 week-old F-IRKO and F-IR/IGFRKO mice (Fig. 3G). Serum AST levels were also elevated in F-IRKO mice at 5 and 12 weeks of age and further increased in F-IRKO and F-IR/IGFRKO mice at 52 weeks of age (Fig. 3H). F-IGFRKO mice did not develop hepatomegaly or increased levels of liver triglycerides, enzymes of de novo lipogenesis, or serum ALT and AST levels.

One-Year-Old Lipodystrophic Mice Develop Liver Inflammation and Fibrosis

By 1 year of age, inflammatory infiltrates were evident in F-IRKO and F-IGFRKO livers on histological examination (Fig. 4A, top panel), and this was confirmed by increased staining using antibody to the macrophage marker F4/80 (Fig. 4A, bottom panel). mRNA expression of *F4/80* and other macrophage and inflammatory markers, including *CD11c* and *Tnf-α*, was also increased three- to eightfold in livers of 1-year-old F-IRKO and F-IR/IGFRKO mice (Fig. 4B), which was not observed at younger ages (Supplementary Fig. 4). Likewise, mRNA expression of fibrogenic genes *aSma*, *Tgf-β*, and *Col1a1* was increased two- to eightfold in 1-year-old F-IRKO and F-IR/IGFRKO mice (Fig. 4C), which again was largely not increased at prior assessments (Supplementary Fig. 5).

At 52 weeks of age, the livers of all F-IRKO and F-IR/IGFRKO mice contained some hepatocytes showing ballooning degeneration, and most exhibited many ballooned hepatocytes, with a ballooning score of 2.0 ± 0.0 and 1.3 ± 0.2, respectively (scale of 0–2, Table 1). At 52 weeks of age, F-IRKO and F-IR/IGFRKO mice showed an increased inflammation score of 0.6 ± 0.2 and 1.5 ± 0.2 (scale 0–3, Table 1), respectively. The most striking histological difference between 12- and 52-week-old mice was seen in the degree of fibrosis. Fibrosis was not present at 12 weeks of age (Table 1); however, at 52 weeks of age, F-IRKO mice showed stage 1 fibrosis, consisting of interstitial and periportal fibrosis, whereas a more severe degree of interstitial fibrosis (stage 3 of 4) was present in F-IR/IGFRKO mice (Fig. 4D and Table 1). Liver inflammation or fibrosis did not develop in F-IGFRKO mice at any age.

One-Year-Old F-IRKO and F-IR/IGFRKO Mice Preserve Some Gluconeogenic Potential

As lipodystrophic mice aged and developed progressive liver disease, their blood glucose levels improved (17). We assessed whether impaired hepatic gluconeogenesis caused by progressive liver disease could be responsible for the improved glucose levels in older mice. On the one hand, mRNA levels of two rate-limiting enzymes of gluconeogenesis, *G6Pase* and *Pepck*, were indeed decreased in the livers of 1-year-old F-IRKO and F-IR/IGFRKO mice.

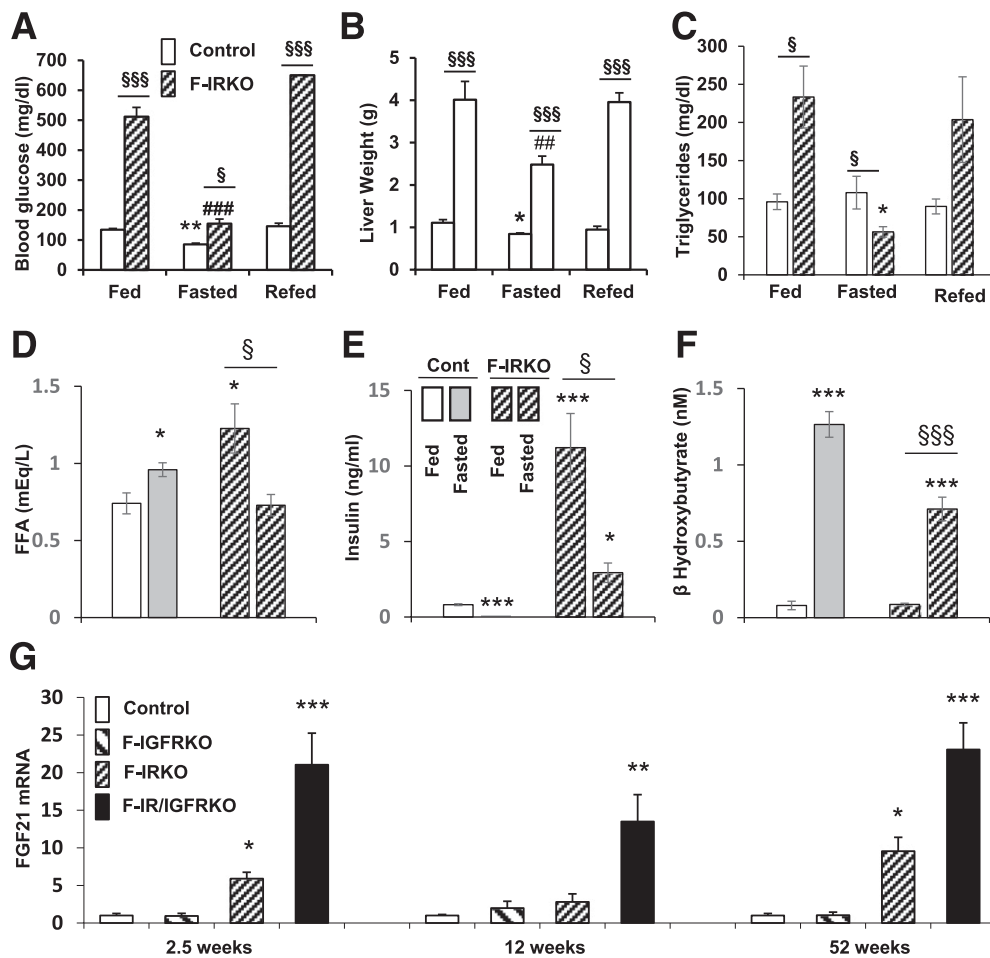


Figure 2—Lipodystrophic mice can mobilize stored liver fat. Blood glucose (A), liver weight (B), serum triglycerides (C), FFAs (D), insulin (E), and β -hydroxybutyrate (F) in 12-week-old random-fed or overnight-fasted control and F-IRKO mice. Results are mean \pm SEM of 9 to 10 animals per group. G: FGF21 mRNA levels in the livers from 2.5-, 12-, and 52-week-old control, F-IGFRKO, F-IRKO, and F-IR/IGFRKO mice. Results are mean \pm SEM of five to eight mice per group. * P < 0.05, ** P < 0.01, and *** P < 0.001 compared with controls; ### P < 0.01 and ### P < 0.001 compared with fed F-IRKO mice; and $\$P$ < 0.05 and $\$\P < 0.001 between adjacent groups.

The expression of other gluconeogenic enzymes, such as *Fbp1* and *Pc*, on the other hand, was elevated (Fig. 5A). Interestingly, the relative expression of gluconeogenic enzymes did not change between 12 and 52 weeks of age, except for *G6pase*, which was elevated in F-IR/IGFRKO mice at 12 weeks but decreased in F-IRKO and F-IR/IGFRKO mice at 52 weeks of age (Fig. 5A). Although the reduction in *G6pase* and *Pepck* expression suggests impaired gluconeogenesis, some gluconeogenic potential was preserved, because 52-week-old F-IRKO and F-IR/IGFRKO mice did not develop hypoglycemia with fasting (Fig. 5B). In addition, F-IRKO and F-IR/IGFRKO mice were able to mobilize stored glucose in response to glucagon and even showed an exaggerated response (Fig. 5C). This is consistent with enhanced glycogen stores in the liver of lipodystrophic mice as assessed by PAS staining (Fig. 5D). Improvement in glucose was also not caused by failure of pancreatic α -cells, because serum glucagon levels were elevated in 52-week-old F-IRKO and F-IR/IGFRKO mice (Fig. 5E).

Liver Tumors Develop in Lipodystrophic Mice at 1 Year of Age

With aging, livers of F-IRKO and F-IR/IGFRKO mice developed gross nodularity (Fig. 6A, top); this occurred in the setting of fibrosis (Fig. 6A, middle, and Supplementary Fig. 6). Histological sections of liver stained for Ki67 showed clusters of proliferating cells in F-IRKO and discrete proliferative nodules in F-IR/IGFRKO livers (Fig. 6A, bottom). These nodules contained hepatocytes with increased mitotic activity and large, atypical nuclei, often with multiple, prominent nucleoli, indicative of severe cellular dysplasia (Supplementary Fig. 7A). Livers of F-IR/IGFRKO mice also contained tumor-like malformations of bile ducts, segments of bone with bone marrow elements, and areas of extramedullary hematopoiesis (Supplementary Fig. 7B–D), as well as increased expression of tumorigenic markers β -catenin, *Afp* and *cyclin D1* (Supplementary Fig. 8A–C). Expression of *Pkm2*, a rate-limiting enzyme of glycolysis, was also increased in F-IR/IGFRKO livers (Fig. 6B). *Pkm2* is normally found

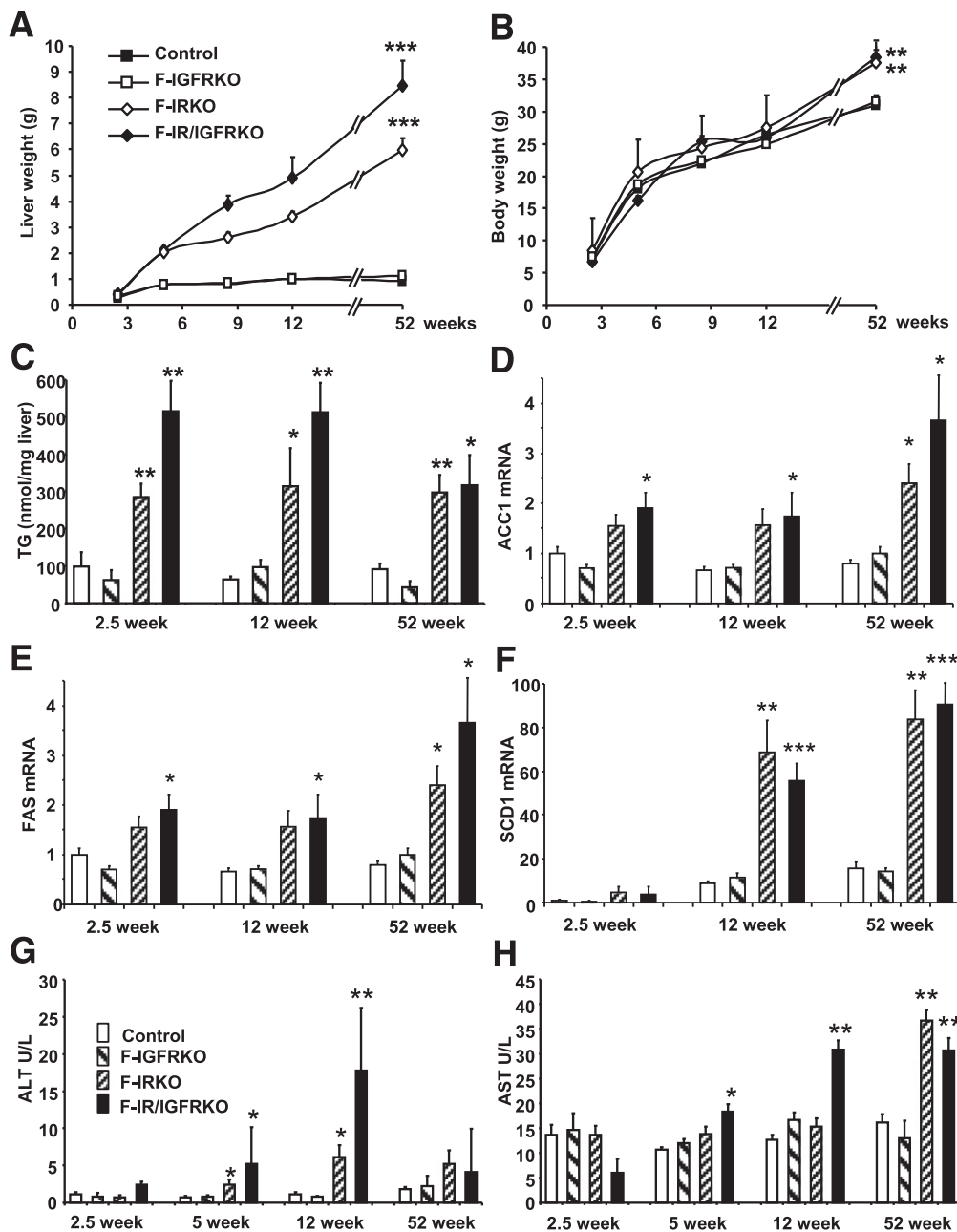


Figure 3—F-IRKO and F-IR/IGFRKO mice develop progressive NAFLD with age. Liver weight (A) and body weight (B) of control, F-IGFRKO, F-IRKO, and F-IR/IGFRKO mice at 2.5, 5, 8, 12, and 52 weeks of age. Results are mean \pm SEM of 12 to 30 animals per group. C: Triglyceride (TG) content was measured in the livers from mice at 2.5, 12, and 52 weeks of age. *Acc1* (D), *Fas* (E), and *Scd1* (F) mRNA expression in control, F-IGFRKO, F-IRKO, and F-IR/IGFRKO mice at 2.5, 12, and 52 weeks of age graphed as a fold-change over controls. Results are mean \pm SEM of five to eight animals per group. Serum ALT (G) and AST (H) levels measured in 2.5-, 5-, 12-, and 52-week-old chow-fed control, F-IGFRKO, F-IRKO, and F-IR/IGFRKO mice. * $P < 0.05$, ** $P < 0.01$, and *** $P < 0.001$ compared with controls.

in tissues with high glycolytic activity, such as embryonic stem cells and tumor cells, but not in mature hepatocytes (24).

Whole-body V_{O_2} was significantly decreased by 30% in 1-year-old F-IRKO and F-IR/IGFRKO mice at least partly because of reduced activity of the mice (Fig. 6C and Supplementary Fig. 9). The respiratory exchange ratio (RER) was also lower in these mice compared with controls at 12 weeks of age, but by 52 weeks of age, the RER was above

0.9 in F-IRKO and F-IR/IGFRKO mice and was actually significantly higher than in controls (Fig. 6C). The latter finding indicates a shift in favor of greater glucose than lipid utilization in the lipodystrophic mice, which is likely from the increased glycolytic activity associated with development of the dysplastic hepatic nodules. IR levels were reduced in the livers of F-IR/IGFRKO mice (Fig. 6D), probably as a result of sustained hyperinsulinemia (25). Also, there was increased serine/threonine p-PTEN,

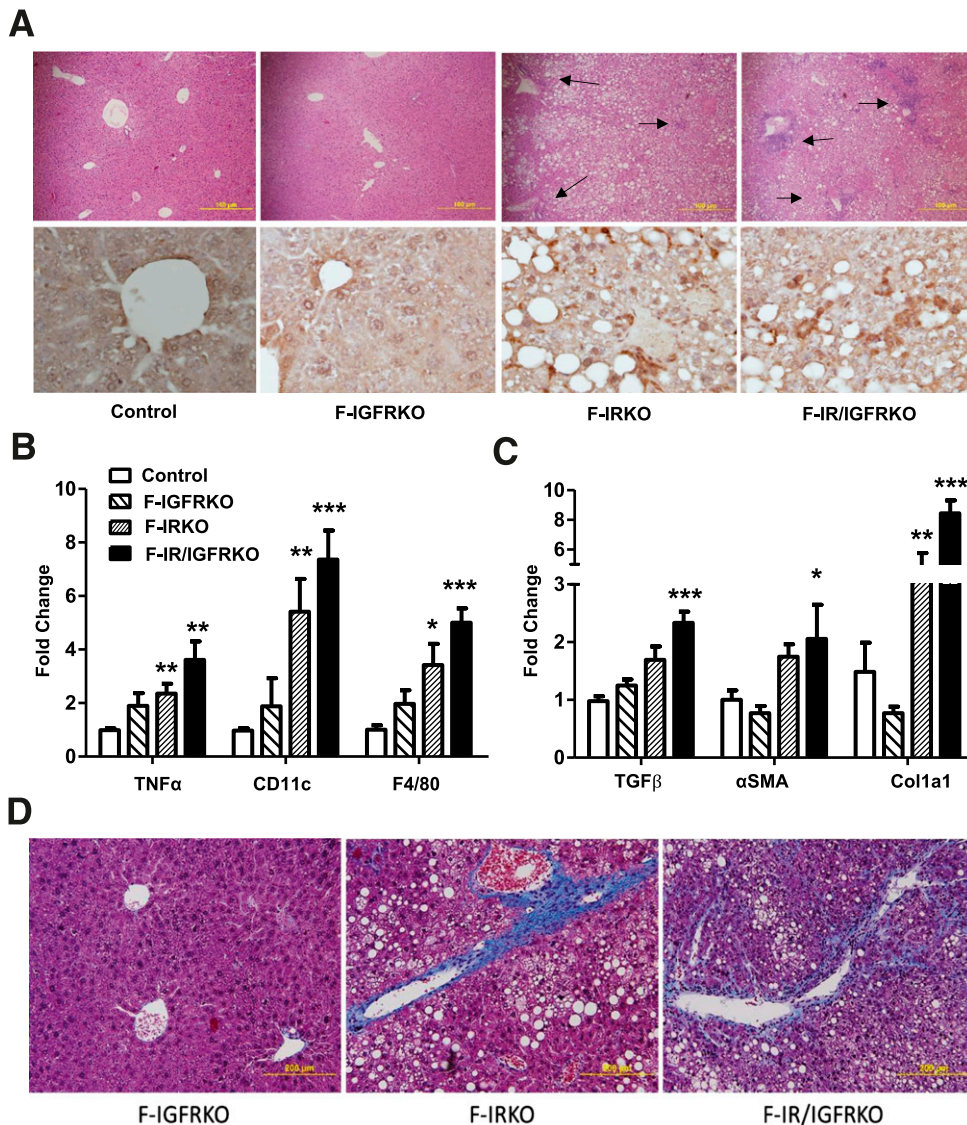


Figure 4—Liver inflammation is apparent at 52 weeks of life. **A:** Liver sections from 52-week-old control, F-IGFRKO, F-IRKO, and F-IR/IGFRKO mice stained with H&E (original magnification $\times 100$) (top panel). Arrows show pockets of inflammation. IHC for macrophage marker F4/80 is shown in the same mice (original magnification $\times 400$) (bottom panel). One representative section from three mice per group is shown. Expression of genes involved in inflammation (**B**) and fibrosis (**C**) in chow-fed control, F-IGFRKO, F-IRKO, and F-IR/IGFRKO mice at 52 weeks of age. Results are mean \pm SEM of four to eight animals per group. * $P < 0.05$, ** $P < 0.01$, and *** $P < 0.001$ compared with controls. **D:** Liver sections from the same mice at 52 weeks of age stained with Masson's trichrome (original magnification $\times 200$). One representative section from four to six mice per group is shown.

decreased total levels of PTEN (Fig. 6D), and increased staining of PIP₃ (Fig. 6E), all consistent with development of hepatic neoplasia.

HFD Accelerates Blood Glucose Normalization

To test to what extent chronic lipotoxicity might be mediating the liver injury and improved glucose levels in aged mice, we fed the HFD (60% fat by calories) to a cohort of 8-week-old control, F-IRKO, and F-IR/IGFRKO mice. Control mice gained weight on the HFD throughout the 12-week study period, whereas F-IR/IGFRKO mice gained body weight initially, but this began to level off after 8 weeks of the diet. F-IRKO mice also initially gained

weight but then started losing body weight after 8 weeks of the diet (Fig. 7A). Likewise, blood glucose levels at 8 weeks on the diet began trending downward, so that at 12 weeks, blood glucose levels of F-IRKO and F-IR/IGFRKO mice were not different from the control mice (Fig. 7B). After 12 weeks of the HFD, glucose tolerance of the lipodystrophic mice also improved and was not different from the control mice (Fig. 7C). Liver histology showed marked steatosis and balloon degeneration in F-IRKO and F-IR/IGFRKO mice, whereas control mice did not develop significant steatosis (Fig. 7D). Liver weight of F-IRKO and F-IR/IGFRKO mice was significantly increased compared with the controls at 12 weeks on the HFD (Fig. 7E), and

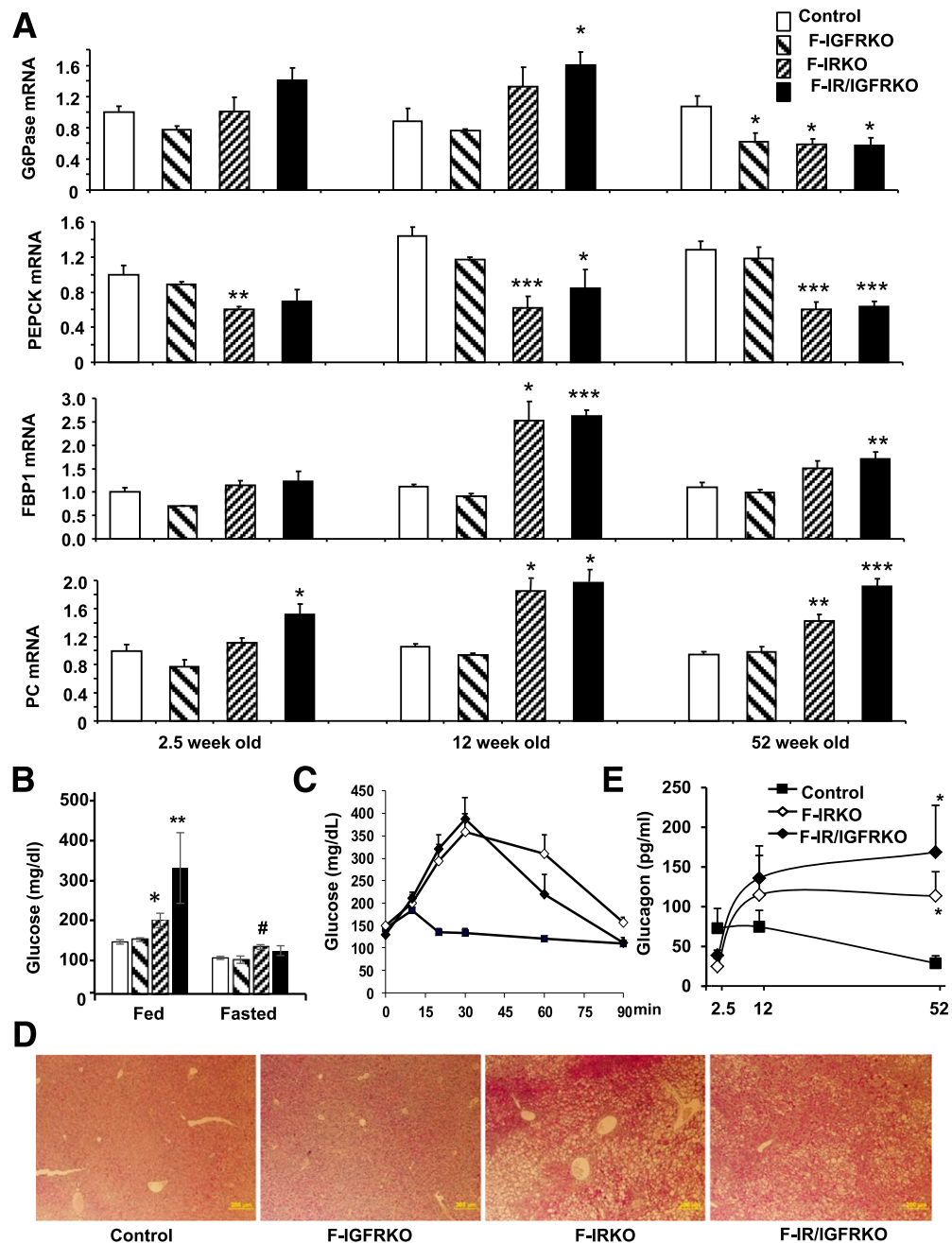


Figure 5—Gluconeogenesis at 52 weeks of age. **A**: mRNA expression of *G6pase*, *Pepck*, *Fbp1*, and *Pc* in control, F-IGFRKO, F-IRKO, and F-IR/IGFRKO mice at the indicated times from 2.5 to 52 weeks of age graphed as fold-change over controls. Results are mean \pm SEM of five to six animals per group. **B**: Random-fed and overnight-fasted blood glucose levels of chow-fed control, F-IGFRKO, F-IRKO, and F-IR/IGFRKO mice at 52 weeks of age. Blood glucose levels (**C**) assessed over 90 min after intraperitoneal glucagon challenge and serum glucagon levels (**E**) in control, F-IRKO, and F-IR/IGFRKO mice at indicated times. Results are mean \pm SEM of five to six animals per group. * $P < 0.05$, ** $P < 0.01$, and *** $P < 0.001$ compared with controls; # $P < 0.05$ compared with fed mice. **D**: PAS-stained liver sections from control, F-IGFRKO, F-IRKO, and F-IR/IGFRKO mice at 52 weeks of age. One representative section from five mice per group is shown.

hepatomegaly was as profound as the liver weight of chow-fed F-IRKO and F-IR/IGFRKO mice at 52 weeks of age.

The expression of gluconeogenic enzymes *G6Pase* and *Pepck* was again decreased in F-IRKO and F-IR/IGFRKO mice (Fig. 7F), similar to the decreased expression of these enzymes at 52 weeks of age on the chow diet. Conversely,

the expression of *Fbp1* was not significantly increased, whereas the mRNA levels of *Pc*, *Gapdh*, *Enol1*, and *Aldo b* were increased in F-IRKO and F-IR/IGFRKO mice (Fig. 7F and Supplementary Fig. 10), suggestive of increased glucose flux. When [14 C]-2-deoxyglucose uptake was assessed in vivo, uptake in the livers of F-IRKO and F-IR/IGFRKO mice tended to be higher, whereas glucose uptake was

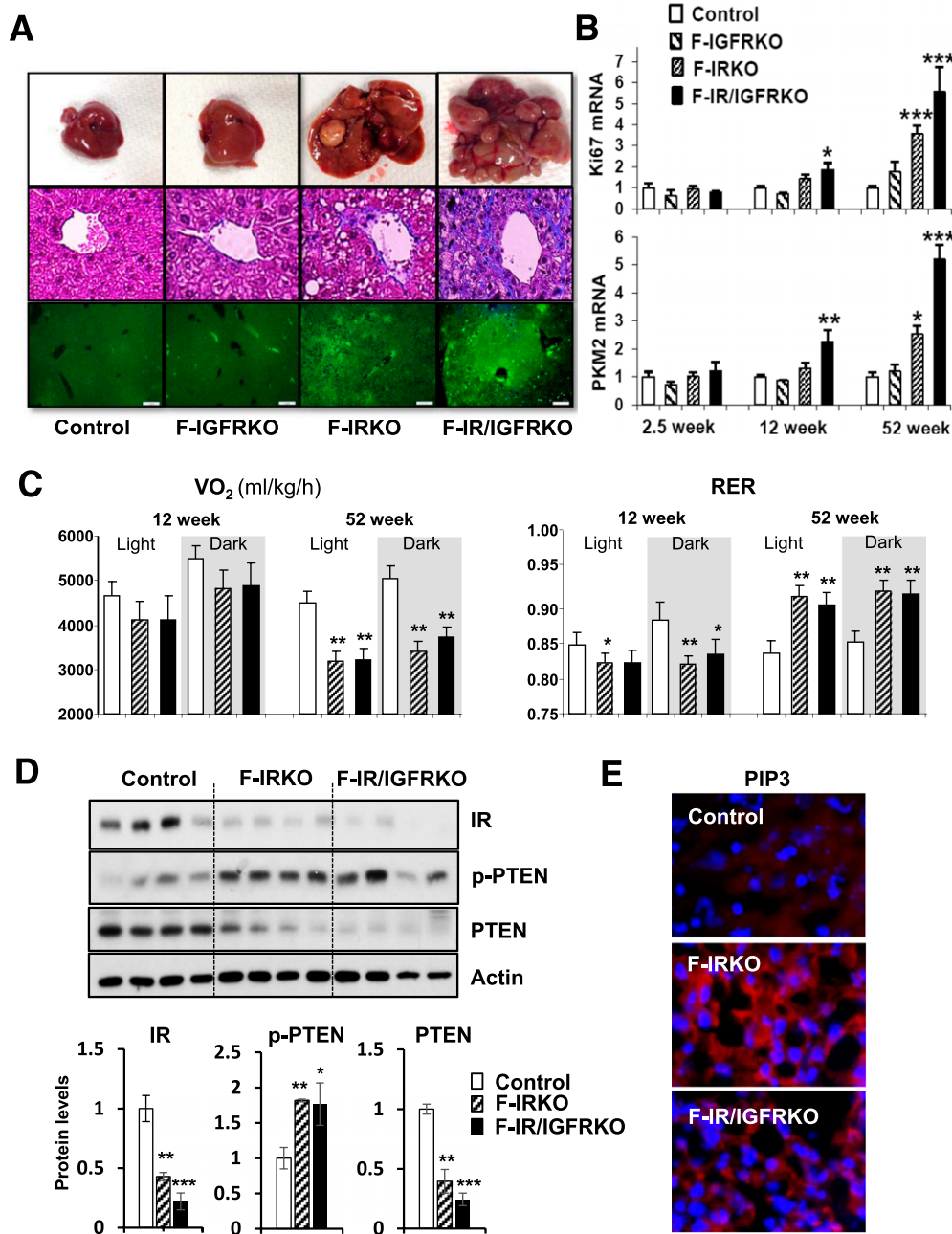


Figure 6—Lipodystrophic mice develop liver tumors and increased glycolysis. **A:** Representative images of whole liver (upper panel), Masson’s trichrome stain (middle panel), and Ki67 staining (lower panel) in 1-year-old control, F-IGFRKO, F-IRKO, and F-IR/IGFRKO mice. Scale bars, 200 μ m. **B:** Ki67 and PKM2 mRNA levels in livers from 2.5-, 12-, and 52-week-old mice. Results are mean \pm SEM of five to eight animals per group. **C:** VO_2 and RER of control, F-IRKO, and F-IR/IGFRKO mice measured in metabolic cages at 12 and 52 weeks of age. Results are mean \pm SEM of 5 to 11 mice per group. **D:** Western blot analysis and densitometric quantification of insulin-signaling molecules from the livers of control, F-IRKO, and F-IR/IGFRKO mice at 1 year of age. Results are mean \pm SEM of four animals per group. **E:** Representative IHC images of PIP₃ in livers of control, F-IRKO, and F-IR/IGFRKO mice at 1 year of age. * $P < 0.05$, ** $P < 0.01$, and *** $P < 0.001$ compared with controls.

decreased in the muscle of F-IR/IGFRKO mice at 12 weeks on the HFD (Supplementary Fig. 11A). Again, normalization of blood glucose levels on the HFD correlated with increased *Pkm2* expression in F-IRKO and F-IR/IGFRKO mice (Fig. 7G). Although these livers did not show gross nodularity, the liver parenchyma was heterogeneous in color (Supplementary Fig. 11B). *FGF21* mRNA levels

were also increased in lipodystrophic mice on the HFD (Fig. 7G), as was the expression of *Acc1*, *Fas*, and *Scd1* (Fig. 7H). The HFD-challenged lipodystrophic mice also developed signs of liver inflammation, with elevated expression of *F4/80*, *Tnf- α* , and *CD11c* (Fig. 7I) and signs of liver fibrosis with elevated *α Sma* and *Colla1* mRNA (Fig. 7J).

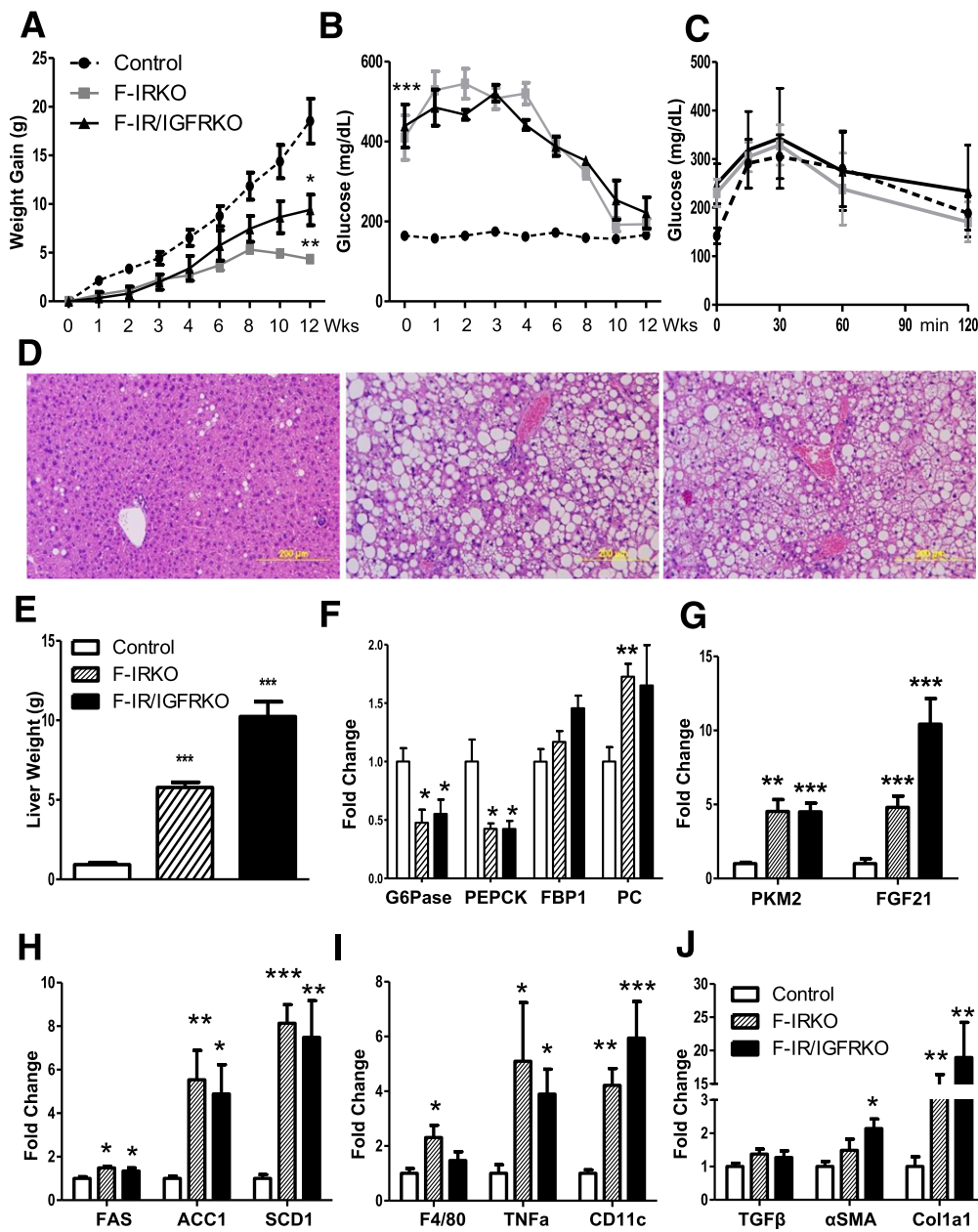


Figure 7—HFD accelerates liver injury in lipodystrophic mice. *A*: Body weight of control, F-IRKO, and F-IR/IGFRKO mice assessed during 12 weeks of HFD feeding. *B*: Blood glucose levels in the same mice assessed at the indicated times. *C*: Glucose tolerance test of control, F-IRKO, and F-IR/IGFRKO mice after 12 weeks of the HFD. Results are mean ± SEM of 6 to 11 animals per group. *D*: H&E-stained liver sections from the same mice. One representative section from six mice per group is shown. *E*: Liver weight of control, F-IRKO, and F-IR/IGFRKO mice after 12 weeks of the HFD. mRNA expression of gluconeogenic enzymes (*F*) and the expression of *Pkm2* and *Fgf21* mRNA (*G*) after 12 weeks of the HFD. mRNA levels of genes involved in de novo lipogenesis (*H*), inflammation (*I*) and fibrosis (*J*) after 12 weeks of the HFD. Results are mean ± SEM of four to six animals per group. **P* < 0.05, ***P* < 0.01, and ****P* < 0.001 compared with controls.

DISCUSSION

In the current study, we show that adipose-specific deletion of IR or combined deletion of IR and IGF1R induces a generalized lipodystrophy phenotype with profound hepatomegaly, marked steatosis, and increased enzymes of de novo lipogenesis. Early on, this results in increased levels of reactive oxygen species in the liver, augmented lipid peroxidation, and hepatocyte balloon degeneration—all

indicative of lipotoxicity. At this age, these mice are able to mobilize stored liver lipids and use different substrates, such that blood glucose levels and liver weight decrease with fasting. Furthermore, lipodystrophic F-IRKO and F-IR/IGFRKO mice are able to robustly increase ketogenesis, perhaps because of increased liver FGF21 expression. Over time, however, lipotoxic effects accumulate, so that lipodystrophic mice develop significant hepatic inflammation and

fibrosis by 52 weeks of age. Interestingly, blood glucose levels also normalize at this age, partly because of chronic lipotoxicity with altered expression of gluconeogenic enzymes and development of highly dysplastic liver nodules that results in greater glucose utilization by liver and a dramatic increase in whole-body RER. Normalization of blood glucose levels can be accelerated by feeding mice an HFD for 12 weeks.

The lipodystrophic syndrome observed in F-IRKO and F-IR/IGFRKO mice is similar to human generalized lipodystrophy in many ways. Both are characterized by low leptin levels, marked insulin resistance, hyperlipidemia, and fatty liver disease (26,27). Leptin replacement reduces blood glucose levels and hepatic steatosis in humans with lipodystrophy (8,10), and leptin replacement also normalizes blood glucose levels in F-IRKO and F-IR/IGFRKO mice (17). The effects of leptin are at partly secondary to reduced food intake and can be mimicked in our lipodystrophic mice with fasting alone.

In humans with generalized lipodystrophy, NAFLD often progresses to NASH and cirrhosis (15), sometimes requiring liver transplantation (14). F-IRKO and F-IR/IGFRKO mice also develop profound and progressive fatty liver disease with massive hepatomegaly (liver weight up to ~25% of body weight), with inflammation, pericellular fibrosis, and an inversion of the ALT-to-AST ratio. Indeed, by 1 year of age, the F-IRKO and F-IR/IGFRKO mice develop overt dysplastic hepatic nodules with severe large-cell dysplasia, frequent mitoses, and elevated tumor markers *Apf* and β -catenin. This is associated with a decrease in liver PTEN levels and increased accumulation of PIP₃, changes that are often seen in liver cancer (28). Thus, the liver injury in our current lipodystrophic model describes a full spectrum of NAFLD progression, including the development of severely dysplastic hepatic nodules.

The liver phenotype in these mice is in contrast to the liver phenotype in our previous study of fat-specific IR and IGF1R deletion driven by *aP2-cre* promoter, which did not develop NAFLD unless challenged with an HFD (18). The difference likely stems from the fact that deletion of IR or IR and IGF1R driven by *aP2-cre* only results in moderately reduced adipose tissue mass, leading to improved glucose tolerance and protection from age-related and hypothalamic lesion-induced obesity (29). Lipodystrophic mice caused by KO of *Srebp1c* using *aP2-cre* also develop NAFLD with progression to NASH, but have not been reported to develop tumors or dysplastic hepatic nodules (30). However, patients with lipodystrophy are known to develop liver adenomas (personal communication from R. Brown and P. Gorden), and hepatocellular carcinoma developed in at least one patient with acquired generalized lipodystrophy (31).

Our findings indicate that stored fat in the liver is a dynamic depot. Lipodystrophic mice lose ~40% of liver weight with fasting and gain 150% above fasted liver weight, after 8 h of refeeding. Canonical thinking is that liver fat accumulation occurs over time and that additive

insults lead to chronic liver injury (32). However, human studies also indicate the dynamic nature of liver fat. As an example, overfeeding for only 3 weeks can increase liver fat by 27%, while total body weight increases by only 2% (33). Furthermore, short-term (2-week) hypocaloric diets are used to reduce liver volume before bariatric surgery (34). In humans, caloric restriction to ~1,100 kcal/day for 48 h can also markedly reduce liver triglyceride content, especially when fed a low-carbohydrate diet (35). Stored liver fat in lipodystrophic mice is used for ketogenesis, which occurs despite the almost complete absence of adipose tissue. This may be caused by elevated liver expression of FGF21, a peptide that regulates lipid metabolism (36) and hepatic ketogenesis (37,38). Thus, liver can function as a fat depot, at least in conditions where adipose tissue does not develop. Extensively relying on the liver for lipid storage does come at a cost, however, because hepatic lipotoxicity is present even at a young age and can be accelerated by HFD feeding.

One of the most unexpected aspects of the F-IRKO and F-IR/IGFRKO phenotype is the improvement in blood glucose levels with aging. The improvement in blood glucose is not because of regeneration of adipose tissue or a reduction in food intake (17). It is also not caused by a return of normal leptin levels or improved insulin sensitivity, because insulin levels remained elevated and pancreatic islets continued to hypertrophy. Instead, the improvement parallels the progression of liver disease from NAFLD to NASH, with inflammation, fibrosis, and severely dysplastic nodules. At least three factors appear to contribute to the improved glycemia:

The first is some impairment in gluconeogenesis caused by chronic liver disease. *Pepck* and *G6Pase* were decreased in livers of 1-year-old F-IRKO and F-IR/IGFRKO mice. Attempts to directly assess gluconeogenesis with a pyruvate challenge, however, resulted in death of the mice, so the extent of impairment is difficult to quantify. Mice tolerated overnight fasting without development of hypoglycemia, and liver glycogen stores were increased.

A second potential contributory factor could have been a failure of pancreatic cells to secrete glucagon or a loss of glucagon receptors in the dysplastic liver. However, serum glucagon levels remained elevated with age, and F-IRKO and F-IR/IGFRKO mice showed a brisk glycemic response to glucagon injection.

The third and perhaps most important factor that could contribute to glucose normalization may be the chronic lipotoxicity and development of severely dysplastic hepatic nodules. Furthermore, expression of PKM2 in whole-liver lysate was increased, contributing to increased glycolysis. This is consistent with the shift from fat to carbohydrate metabolism with aging, as exemplified by the increase in whole-body RER. Lipotoxicity likely mediates the liver injury because HFD feeding accelerates blood glucose normalization. This occurred even without gross evidence of tumor development; however, the key enzyme of glycolysis, PKM2, is profoundly increased in

the lipodystrophic mice after only 12 weeks of HFD feeding. Hyperinsulinemia may directly increase PKM2 levels (39) and thus may lead to glucose normalization in the absence of highly dysplastic liver nodules.

In summary, F-IRKO and F-IR/IGFRKO mice provide a unique new model to study the development and progression of fatty liver disease. Using this model, we show that lipodystrophic mice develop a full spectrum of NAFLD, which progresses to NASH, fibrosis, and ultimately, highly dysplastic liver nodules, which is associated with improvement in blood glucose levels. This liver injury can be accelerated by feeding mice an HFD. Taken together, these data indicate that lipotoxicity can play a major role in the development of liver disease. This can then contribute to altered whole-body metabolism, modifying disease pathogenesis in unexpected ways.

Funding. This work was supported by the Joslin Diabetes and Endocrinology Research Center Core Laboratories (P30-DK-036836) and by National Institute of Diabetes and Digestive and Kidney Diseases grants K12-HD-000850 to S.S. and R01-DK-031036 and R01-DK-082659 to C.R.K. M.H.S. was partly supported by funds from the University of Bergen, KG Jebsen Foundation, Norwegian Society of Endocrinology, Eckbo's Foundation, the T. Wilhelmsen Foundation, and the Norwegian Diabetes Association. The Sunstar Foundation supported S.F.

Duality of Interest. No potential conflicts of interest relevant to this article were reported.

Author Contributions. S.S. and J.B. generated the data and wrote the manuscript. M.H.S., S.F., M.-F.H., E.P.H., J.W., and A.R.P.-A. generated the data and reviewed the manuscript. C.R.K. oversaw the project, contributed to discussion, and helped write the manuscript. C.R.K. is the guarantor of this work and, as such, had full access to all the data in the study and takes responsibility for the integrity of the data and the accuracy of the data analysis.

References

- He W, Barak Y, Hevener A, et al. Adipose-specific peroxisome proliferator-activated receptor gamma knockout causes insulin resistance in fat and liver but not in muscle. *Proc Natl Acad Sci U S A* 2003;100:15712–15717
- Moitra J, Mason MM, Olive M, et al. Life without white fat: a transgenic mouse. *Genes Dev* 1998;12:3168–3181
- Pajvani UB, Trujillo ME, Combs TP, et al. Fat apoptosis through targeted activation of caspase 8: a new mouse model of inducible and reversible lipodystrophy. *Nat Med* 2005;11:797–803
- Shimomura I, Hammer RE, Richardson JA, et al. Insulin resistance and diabetes mellitus in transgenic mice expressing nuclear SREBP-1c in adipose tissue: model for congenital generalized lipodystrophy. *Genes Dev* 1998;12:3182–3194
- Chalasanani N, Younossi Z, Lavine JE, et al.; American Gastroenterological Association; American Association for the Study of Liver Diseases; American College of Gastroenterology. The diagnosis and management of non-alcoholic fatty liver disease: practice guideline by the American Gastroenterological Association, American Association for the Study of Liver Diseases, and American College of Gastroenterology. *Gastroenterology* 2012;142:1592–1609
- Gorden P, Lupsa BC, Chong AY, Lungu AO. Is there a human model for the 'metabolic syndrome' with a defined aetiology? *Diabetologia* 2010;53:1534–1536
- Haque WA, Shimomura I, Matsuzawa Y, Garg A. Serum adiponectin and leptin levels in patients with lipodystrophies. *J Clin Endocrinol Metab* 2002;87:2395
- Safar Zadeh E, Lungu AO, Cochran EK, et al. The liver diseases of lipodystrophy: the long-term effect of leptin treatment. *J Hepatol* 2013;59:131–137
- Simha V, Szczepaniak LS, Wagner AJ, DePaoli AM, Garg A. Effect of leptin replacement on intrahepatic and intramyocellular lipid content in patients with generalized lipodystrophy. *Diabetes Care* 2003;26:30–35
- Petersen KF, Oral EA, Dufour S, et al. Leptin reverses insulin resistance and hepatic steatosis in patients with severe lipodystrophy. *J Clin Invest* 2002;109:1345–1350
- Robbins DC, Sims EA. Recurrent ketoacidosis in acquired, total lipodystrophy (lipoatrophic diabetes). *Diabetes Care* 1984;7:381–385
- Domingo P, Gallego-Escuredo JM, Domingo JC, et al. Serum FGF21 levels are elevated in association with lipodystrophy, insulin resistance and biomarkers of liver injury in HIV-1-infected patients. *AIDS* 2010;24:2629–2637
- Spolcová A, Holubová M, Mikulášková B, et al. Changes in FGF21 serum concentrations and liver mRNA expression in an experimental model of complete lipodystrophy and insulin-resistant diabetes. *Physiol Res* 2014;63:483–490
- Cauble MS, Gilroy R, Sorrell MF, et al. Lipoatrophic diabetes and end-stage liver disease secondary to nonalcoholic steatohepatitis with recurrence after liver transplantation. *Transplantation* 2001;71:892–895
- Javor ED, Ghany MG, Cochran EK, et al. Leptin reverses nonalcoholic steatohepatitis in patients with severe lipodystrophy. *Hepatology* 2005;41:753–760
- Schneeweiss B, Pammer J, Ratheiser K, et al. Energy metabolism in acute hepatic failure. *Gastroenterology* 1993;105:1515–1521
- Boucher J, Softic S, El Ouaamari A, et al. Differential roles of insulin and IGF-1 receptors in adipose tissue development and function. *Diabetes* 2016;65:2201–2213
- Boucher J, Mori MA, Lee KY, et al. Impaired thermogenesis and adipose tissue development in mice with fat-specific disruption of insulin and IGF-1 signalling. *Nat Commun* 2012;3:902
- Debosch BJ, Chen Z, Saben JL, Finck BN, Moley KH. Glucose transporter 8 (GLUT8) mediates fructose-induced de novo lipogenesis and macrosteatosis. *J Biol Chem* 2014;289:10989–10998
- O'Neill BT, Lauritzen HP, Hirshman MF, Smyth G, Goodyear LJ, Kahn CR. Differential role of insulin/IGF-1 receptor signaling in muscle growth and glucose homeostasis. *Cell Reports* 2015;11:1220–1235
- Eguchi J, Wang X, Yu S, et al. Transcriptional control of adipose lipid handling by IRF4. *Cell Metab* 2011;13:249–259
- Mannaerts I, Schroyen B, Verhulst S, et al. Gene expression profiling of early hepatic stellate cell activation reveals a role for Igfbp3 in cell migration. *PLoS One* 2013;8:e84071
- Gramlich T, Kleiner DE, McCullough AJ, Matteoni CA, Boparai N, Younossi ZM. Pathologic features associated with fibrosis in nonalcoholic fatty liver disease. *Hum Pathol* 2004;35:196–199
- Carter-Kent C, Brunt EM, Yerian LM, et al. Relations of steatosis type, grade, and zonality to histological features in pediatric nonalcoholic fatty liver disease. *J Pediatr Gastroenterol Nutr* 2011;52:190–197
- Soli AH, Kahn CR, Neville DM Jr, Roth J. Insulin receptor deficiency in genetic and acquired obesity. *J Clin Invest* 1975;56:769–780
- Huang-Doran I, Sleight A, Rochford JJ, O'Rahilly S, Savage DB. Lipodystrophy: metabolic insights from a rare disorder. *J Endocrinol* 2010;207:245–255
- Fiorenza CG, Chou SH, Mantzoros CS. Lipodystrophy: pathophysiology and advances in treatment. *Nat Rev Endocrinol* 2011;7:137–150
- Horie Y, Suzuki A, Kataoka E, et al. Hepatocyte-specific Pten deficiency results in steatohepatitis and hepatocellular carcinomas. *J Clin Invest* 2004;113:1774–1783
- Blüher M, Michael MD, Peroni OD, et al. Adipose tissue selective insulin receptor knockout protects against obesity and obesity-related glucose intolerance. *Dev Cell* 2002;3:25–38
- Nakayama H, Otake S, Ueno T, et al. Transgenic mice expressing nuclear sterol regulatory element-binding protein 1c in adipose tissue exhibit liver histology similar to nonalcoholic steatohepatitis. *Metabolism* 2007;56:470–475
- Misra A, Garg A. Clinical features and metabolic derangements in acquired generalized lipodystrophy: case reports and review of the literature. *Medicine (Baltimore)* 2003;82:129–146

32. Day CP, James OF. Steatohepatitis: a tale of two "hits"? *Gastroenterology* 1998;114:842–845
33. Sevastianova K, Santos A, Kotronen A, et al. Effect of short-term carbohydrate overfeeding and long-term weight loss on liver fat in overweight humans. *Am J Clin Nutr* 2012;96:727–734
34. van Wissen J, Bakker N, Doodeman HJ, Jansma EP, Bonjer HJ, Houdijk AP. Preoperative methods to reduce liver volume in bariatric surgery: a systematic review. *Obes Surg* 2016;26:251–256
35. Kirk E, Reeds DN, Finck BN, Mayurranjan SM, Patterson BW, Klein S. Dietary fat and carbohydrates differentially alter insulin sensitivity during caloric restriction. *Gastroenterology* 2009;136:1552–1560
36. Murata Y, Konishi M, Itoh N. FGF21 as an endocrine regulator in lipid metabolism: from molecular evolution to physiology and pathophysiology. *J Nutr Metab* 2011;2011:981315
37. Inagaki T, Dutchak P, Zhao G, et al. Endocrine regulation of the fasting response by PPARalpha-mediated induction of fibroblast growth factor 21. *Cell Metab* 2007;5:415–425
38. Badman MK, Pissios P, Kennedy AR, Koukos G, Flier JS, Maratos-Flier E. Hepatic fibroblast growth factor 21 is regulated by PPARalpha and is a key mediator of hepatic lipid metabolism in ketotic states. *Cell Metab* 2007;5:426–437
39. Iqbal MA, Siddiqui FA, Gupta V, et al. Insulin enhances metabolic capacities of cancer cells by dual regulation of glycolytic enzyme pyruvate kinase M2. *Mol Cancer* 2013;12:72
40. Kleiner DE, Brunt EM, Van Natta M, et al.; Nonalcoholic Steatohepatitis Clinical Research Network. Design and validation of a histological scoring system for nonalcoholic fatty liver disease. *Hepatology* 2005;41:1313–1321